

Supplementary Material

**The role of herbivory in shaping dryland
vegetation ecosystem: linking spiral vegetation
patterns and nonlinear-nonlocal grazing**

Mrinal Kanti Pal¹, Swarup Poria¹

¹Department of Applied Mathematics,
University of Calcutta,
92 APC Road, Kolkata-700009, India.

Corresponding author: mrinalkantipal13@gmail.com

March 30, 2023

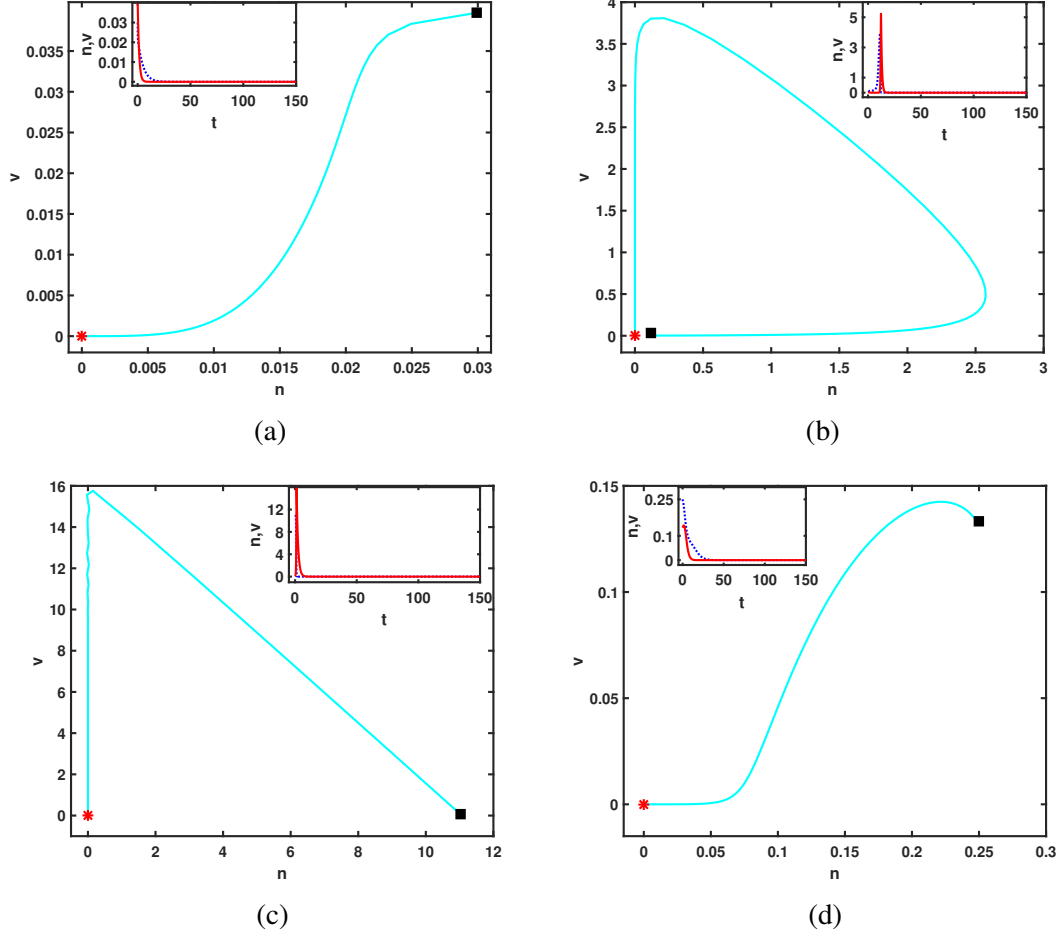


Figure 1: Phase portrait and time-series of system (3) with Type II grazing at a particular grid position (considered $(0,0)$ spatial point in computational domain $\Omega = [-40, 40] \times [-40, 40]$ ($\approx 1 \text{ m}^2$)), $D = 3.2$. The trajectory (cyan line) starts at a point (black square) near HSS (a) $E_0(0,0)$, (b) $E_1(0.9075,0)$, (c) $E_2(11.01925,0)$, (d) $E_3(0.22222,0.084544)$ and ends at the point marked by red asterisk. The time-series evaluations are shown in the inset figures, the blue (dotted) and red line represents vegetation biomass and grazing field respectively.

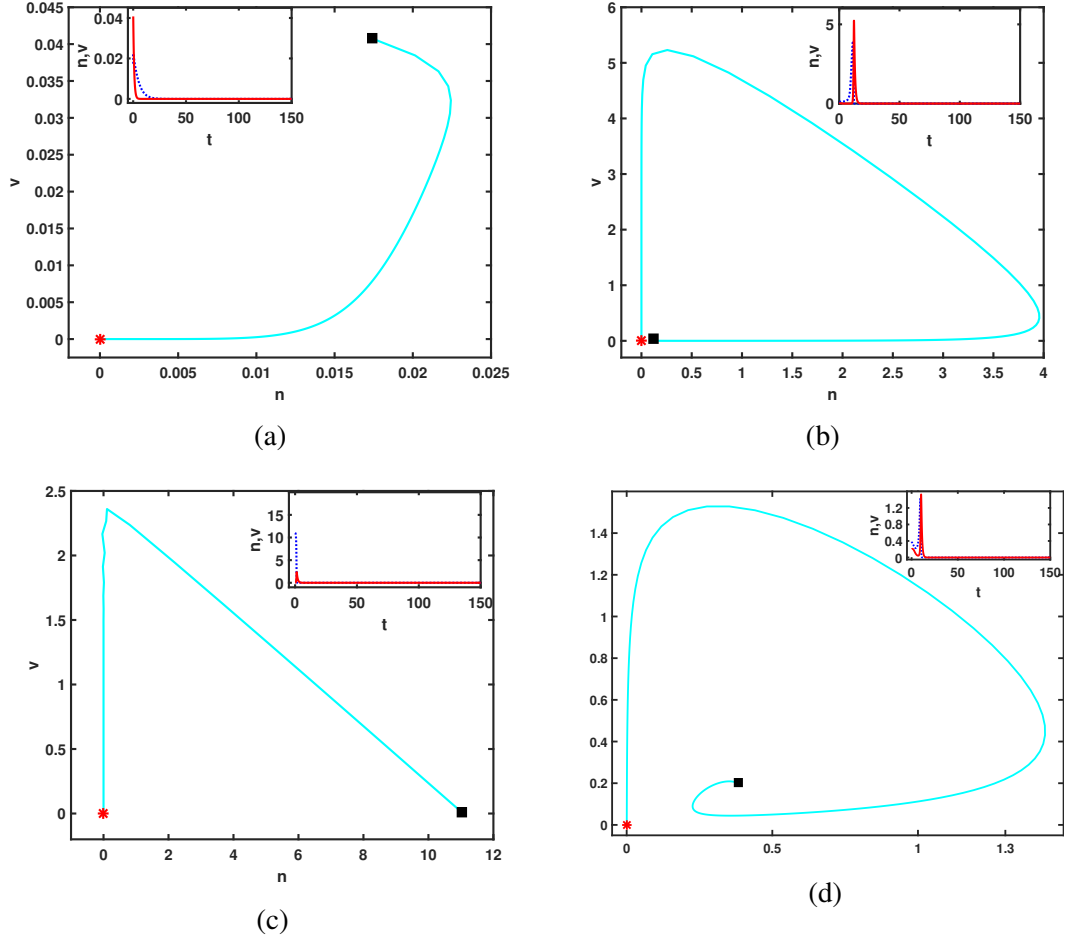


Figure 2: Same as Figure 1 for Type II, $D = 4.8$. The trajectory (cyan line) starts at a point (black square) near HSS (a) $E_0(0,0)$, (b) $E_1(0.9075,0)$, (c) $E_2(11.01925,0)$, (d) $E_3(0.352941, 0.164570)$.

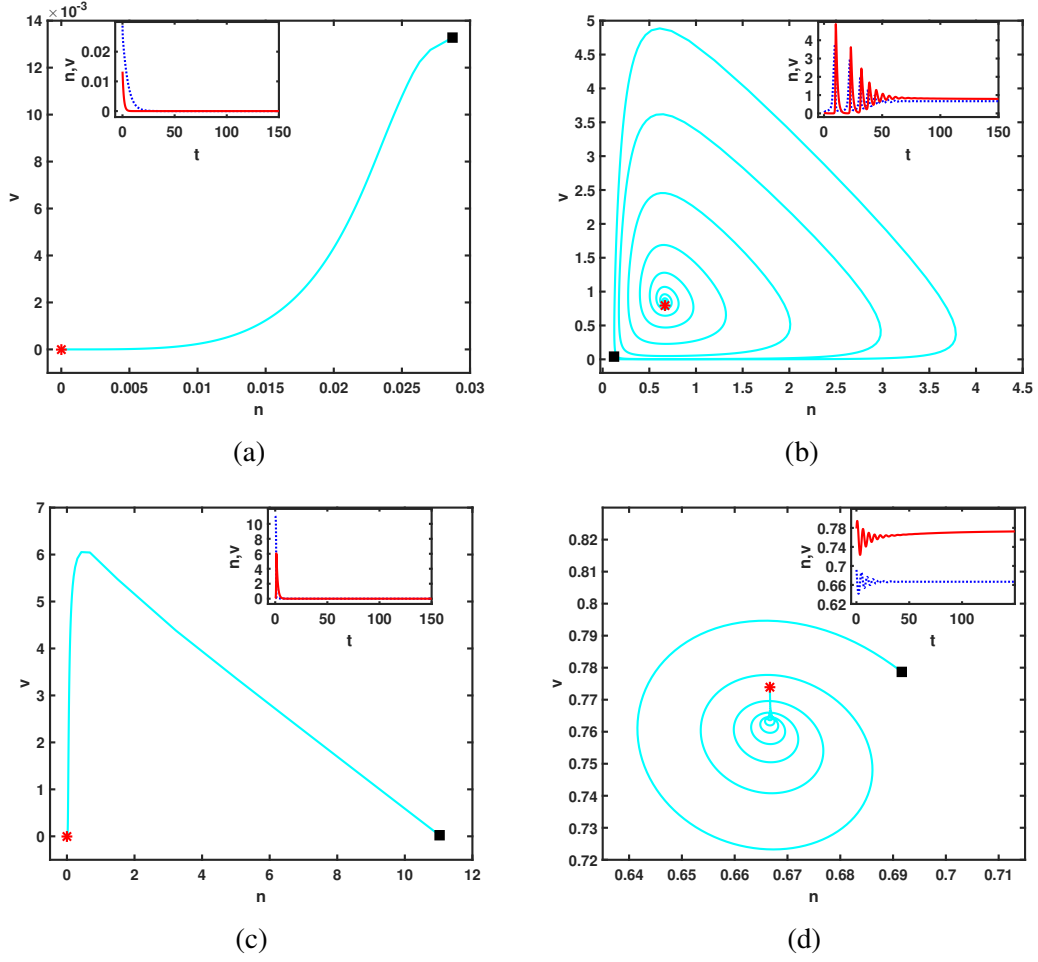


Figure 3: Same as Figure 1 for Type III, $D = 3.2$. The trajectory (cyan line) starts at a point (black square) near HSS (a) $E_0(0,0)$, (b) $E_1(0.9075,0)$, (c) $E_2(11.01925,0)$, (d) $E_3(0.66666,0.773942)$.

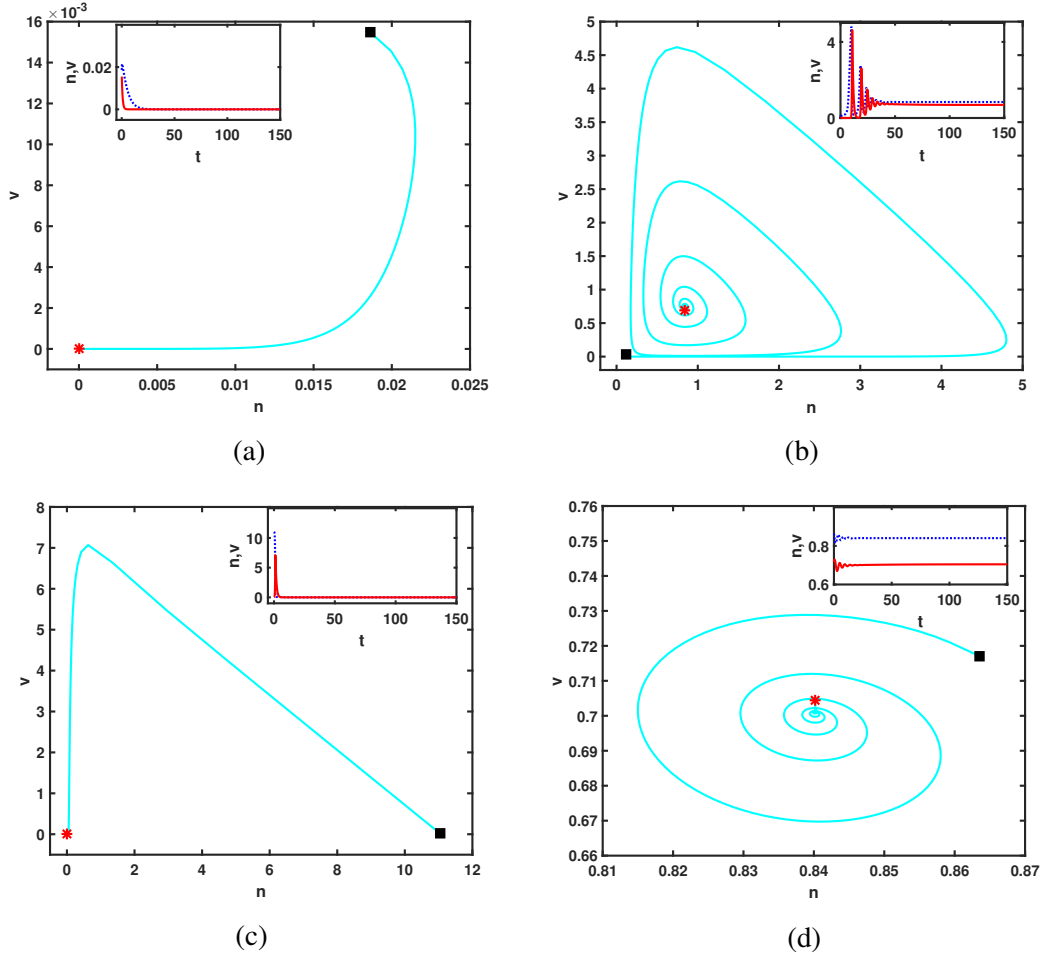


Figure 4: Same as Figure 1 for Type III, $D = 4.8$. The trajectory (cyan line) starts at a point (black square) near HSS (a) $E_0(0,0)$, (b) $E_1(0.9075,0)$, (c) $E_2(11.01925,0)$, (d) $E_3(0.352941,0.164570)$.

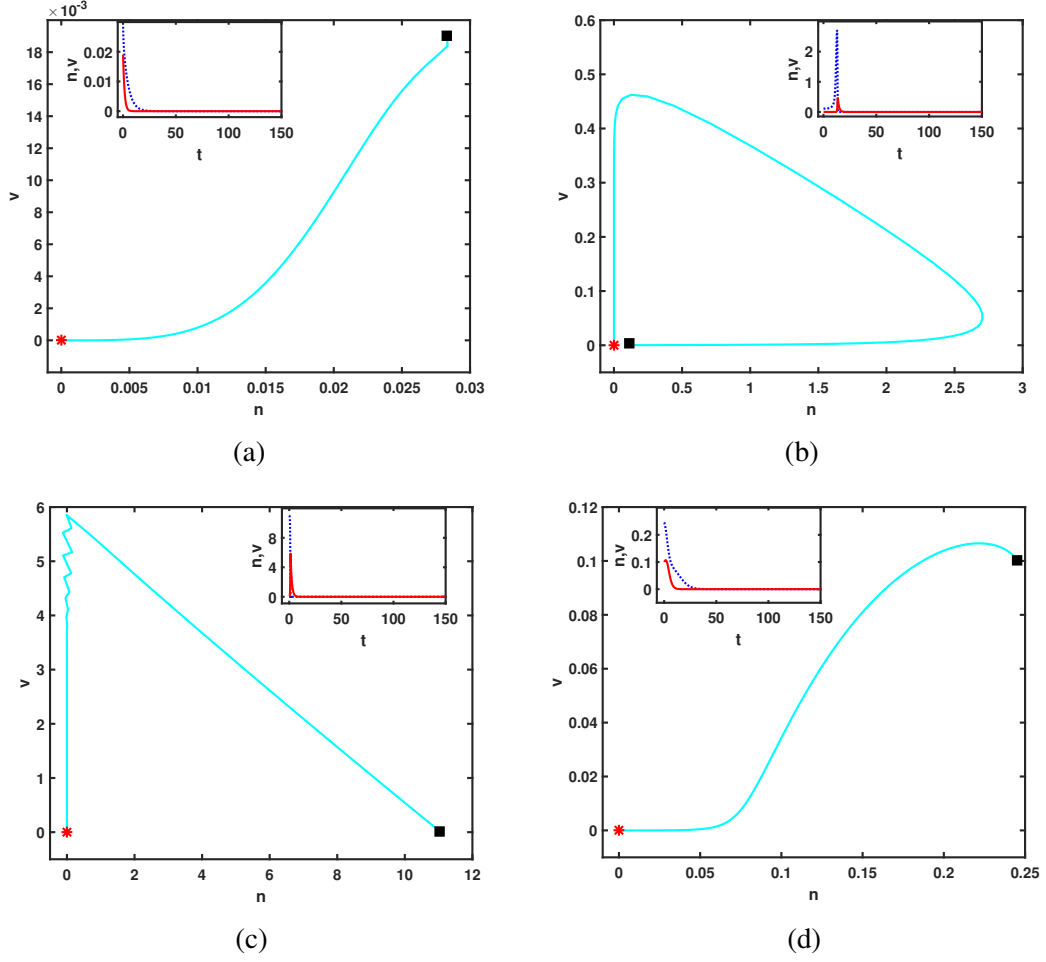
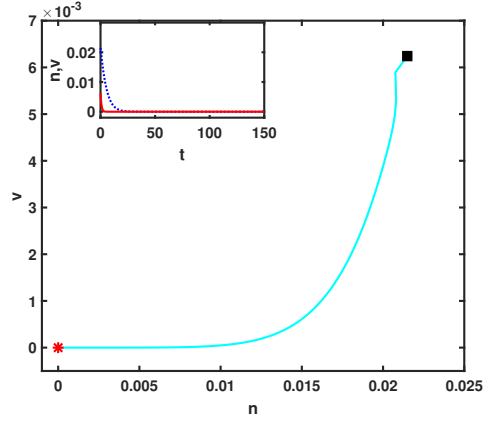
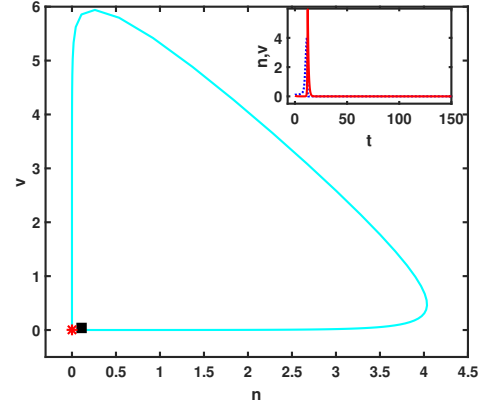


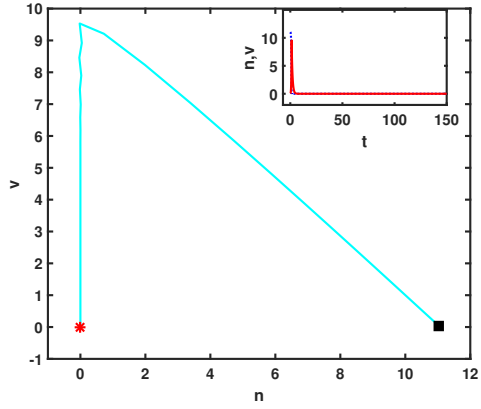
Figure 5: Phase portrait and time-series of system (4) with Type II grazing at a particular grid position (considered $(0,0)$ spatial point in computational domain $\Omega = [-40, 40] \times [-40, 40]$ ($\approx 1 \text{ m}^2$)), $D = 3.2$. The trajectory (cyan line) starts at a point (black square) near HSS (a) $E_0(0,0)$, (b) $E_1(0.9075,0)$, (c) $E_2(11.01925,0)$, (d) $E_3(0.66666,0.773942)$.



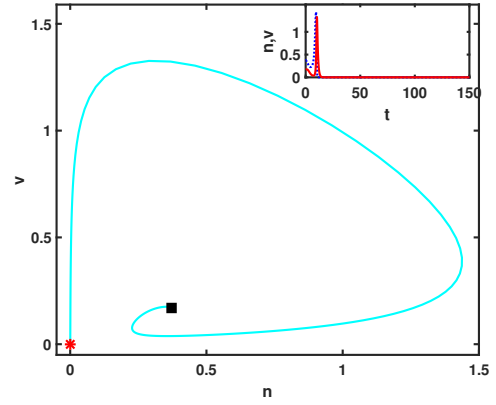
(a)



(b)



(c)



(d)

Figure 6: Same as Figure 5 for Type II, $D = 4.8$. The trajectory (cyan line) starts at a point (black square) near HSS(a) $E_0(0,0)$, (b) $E_1(0.9075,0)$, (c) $E_2(11.01925,0)$, (d) $E_3(0.352941,0.164570)$.

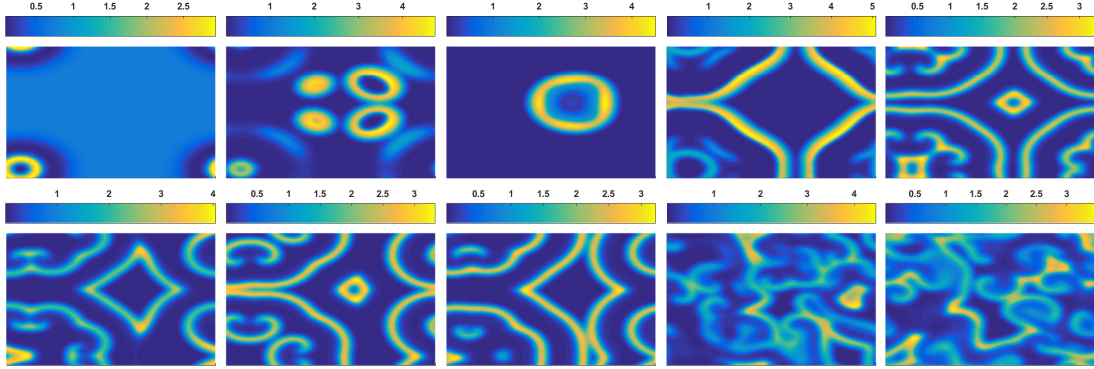


Figure 7: Snapshots of vegetation biomass n taken at different instances as the numerical simulation of model (4) with Type III grazing goes on (time is increasing from left to right row wise: $t = 50, 100, 150, 200, 250, 300, 350, 400, 450, 500$). The horizontal and vertical direction of each plot are the x_1 and x_2 axis respectively; here computational domain is $\Omega = [-40, 40] \times [-40, 40]$ ($\approx 1 \text{ m}^2$) and $D = 3.2$. Initial Condition: A homogeneous vegetation cover with $u = u_3, v = v_3$ all over the domain except a small spot where a random and in-homogeneous perturbation (in range of $(0, 0.05)$) is added to it.

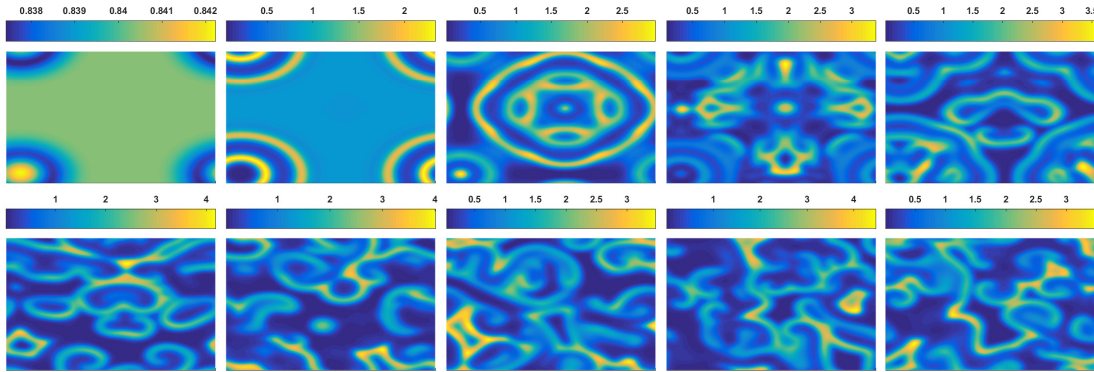


Figure 8: Same setting as Figure 7, except here $D = 4.8$ instead of $D = 3.2$.